Dwarf galaxies in the MATLAS survey: The satellite system of NGC 474 under scrutiny with MUSE

Oliver Müller, Francine R Marleau, Nick Heesters, Pierre-Alain Duc, Marcel S Pawlowski, Mélina Poulain, Rebecca Habas, Elisabeth Sola, Mathias Urbano, Rory Smith, et al.

A&A, 693, A44 (2025)
https://doi.org/10.1051/0004-6361/202450143

Astronomy & Astrophysics

Dwarf galaxies in the MATLAS survey: The satellite system of NGC 474 under scrutiny with MUSE

Oliver Müller[1,⋆], Francine R. Marleau[2], Nick Heesters[1], Pierre-Alain Duc[3], Marcel S. Pawlowski[4], Mélina Poulain[5], Rebecca Habas[6], Elisabeth Sola[7], Mathias Urbano[3], Rory Smith[8], Patrick Durrell[9], Eric Emsellem[10], Rubén Sánchez-Janssen[11], Sungsoon Lim[12], and Sanjaya Paudel[12]

[1] Institute of Physics, Laboratory of Astrophysics, Ecole Polytechnique Fédérale de Lausanne (EPFL), 1290 Sauverny, Switzerland
[2] Institut für Astro- und Teilchenphysik, Universität Innsbruck, Technikerstraße 25/8, Innsbruck A-6020, Austria
[3] Observatoire Astronomique de Strasbourg (ObAS), Université de Strasbourg – CNRS, UMR 7550, Strasbourg, France
[4] Leibniz-Institut für Astrophysik Potsdam (AIP), An der Sternwarte 16, D-14482 Potsdam, Germany
[5] Space Physics and Astronomy Research Unit, University of Oulu, PO Box 3000, FI-90014 Oulu, Finland
[6] INAF – Astronomical Observatory of Abruzzo, Via Maggini, 64100 Teramo, Italy
[7] Institute of Astronomy, Madingley Rd, Cambridge CB3 0HA, UK
[8] Departamento de Física, Universidad Técnica Federico Santa María, Santiago, Chile
[9] Youngstown State University, One University Plaza, Youngstown, OH 44555, USA
[10] European Southern Observatory, Karl-Schwarzschild Straße 2, D-85748 Garching bei München, Germany
[11] UK Astronomy Technology Centre, Royal Observatory, Blackford Hill, Edinburgh EH9 3HJ, UK
[12] Department of Astronomy and Center for Galaxy Evolution Research, Yonsei University, Seoul 03722, South Korea

Received 27 March 2024 / Accepted 11 November 2024

ABSTRACT

A recent study of the distribution of dwarf galaxies in the MATLAS sample in galaxy groups revealed an excess of flattened satellite structures, reminiscent of the co-rotating planes of dwarf galaxies discovered in the local Universe. If confirmed, this lends credence to the plane-of-satellite problem and further challenges the standard model of hierarchical structure formation. However, with only photometric data and no confirmation of the satellite membership, the study could not address the plane-of-satellite problem in full detail. Here we present spectroscopic follow-up observations of one of the most promising planes-of-satellite candidates in the MATLAS survey, the satellite system of NGC 474. Employing MUSE at the VLT and full spectrum fitting, we studied 13 dwarf galaxy candidates and confirmed nine to be members of the field around NGC 474. Measuring the stellar populations of all observed galaxies, we find that the MATLAS dwarfs have lower metallicities than the Local Group dwarfs at a given luminosity. Two dwarf galaxies may form a pair of satellites based on their close projection and common velocity. Within the virial radius, we do not find a significant plane-of-satellites, however, there is a sub-population of six dwarf galaxies which seem to be anti-correlated in phase-space. Due to the low number of dwarf galaxies, this signal may arise by chance. With over 2000 dwarf galaxy candidates found in the MATLAS survey, this remains an intriguing data set to study the plane-of-satellites problem in a statistical fashion once more follow-up observations have been conducted.

Key words. galaxies: distances and redshifts – galaxies: dwarf – galaxies: groups: individual: NGC 474 – galaxies: kinematics and dynamics – large-scale structure of Universe

1. Introduction

The arrangement and movement patterns of dwarf galaxies surrounding both the Milky Way and the Andromeda galaxy have ignited a continuous debate regarding their compatibility with the prevailing Λ+cold dark matter (ΛCDM) standard cosmological model (e.g., Kroupa et al. 2005; Libeskind et al. 2007; Pawlowski & Kroupa 2013; Wang et al. 2013; Ibata et al. 2014a; Gillet et al. 2015; Cautun et al. 2015a,b; Buck et al. 2016; Fernando et al. 2017; Pawlowski 2021; Sales et al. 2022; Santos-Santos et al. 2023; Sato & Chiba 2024; Gámez-Marín et al. 2024). Numerous studies over five decades (e.g., Lynden-Bell 1976; McConnachie & Irwin 2006; Koch & Grebel 2006; Metz et al. 2008; Pawlowski et al. 2012; Ibata et al. 2013; Conn et al. 2013; Sohn et al. 2020; Taibi et al. 2024; Júlio et al. 2024) have explored these observations, with a particular focus on the satellite systems' structure and kinematics. Today, this debate has been dubbed the plane-of-satellites problem, and in short describes that the dwarf galaxies are arranged in thin, planar-like structures, in which they seem to co-orbit around their host galaxies (see Pawlowski 2018, 2021 for reviews). This is in stark contrast to the more pressure supported halos found in cosmological simulations.

Satellite systems are pivotal tests of ΛCDM, as their dynamics are primarily governed by gravitational forces on scales of hundreds of kiloparsecs, mostly unaffected by internal baryonic processes (Pawlowski 2018; Müller et al. 2018a). Consequently, numerous research teams have extended their investigations beyond the Local Group, exploring analogous structures. Beyond the Local Group, claims of flattened distributions have been proposed around several giant galaxies (Chiboucas et al. 2013; Müller et al. 2017, 2018b, 2024; Martínez-Delgado et al. 2021; Paudel et al. 2021; Crosby et al. 2023; Mutlu-Pakdil et al. 2024; Karachentsev & Kroupa 2024; Pawlowski et al. 2024). The best studied of these is the lenticular galaxy Cen A and its satellite system, which exhibits a statistically significant correlation in phase-space (Tully et al. 2015; Müller et al. 2016, 2018a, 2019, 2021a; Kanehisa et al. 2023). Intriguingly, these flattened

⋆ Corresponding author; oliver.muller@epfl.ch

structures often align with the local cosmic web, suggesting a potential common formation scenario for such configurations (Libeskind et al. 2015, 2019; Müller et al. 2024).

While many surveys target individual galaxies, the Mass Assembly of early-Type GaLAxies with their fine Structures (MATLAS, Duc et al. 2015; Bílek et al. 2020) survey[1] observed a total of 180 early type galaxies in the nearby universe employing MegaCam at CFHT to a limiting surface brightness magnitude of ≈28.5 mag/arcsec^2. Over 2000 dwarf galaxies were discovered surrounding these giants (Habas et al. 2020; Poulain et al. 2021), enabling the statistical analysis of their satellite systems. From a subsample of 119 satellite systems, Heesters et al. (2021) identified a statistically significant population of 31 flattened dwarf structures, based on their on-sky positions. This analysis, however, could not take into account any velocity trend, because the necessary observations were not available at the time. It is a time consuming task to get spectroscopy of the mostly quiescent dwarf galaxies, needing 8m class telescopes and long exposures (e.g., Danieli et al. 2019; Müller et al. 2020; Heesters et al. 2023; Ferré-Mateu et al. 2023), and to complete a full dwarf satellite system requires hours of dedicated observations.

A further issue in the analysis of the MATLAS fields was that most of the dwarf galaxy candidates did not have a confirmed membership status, meaning that the measurement of the flattening was based on the assumption that all candidates were satellites of the central galaxy. This may not be the case, as Heesters et al. (2023) showed that only 75% of a subsample of 56 MATLAS dwarf galaxy candidates were confirmed to be actual members of their putative hosts through follow-up observations. This implies that the identified flattened structures in Heesters et al. (2021) can have spurious members and the observed satellite distribution may change depending of membership confirmation and rejection.

In this paper, we present the first follow-up observation of an almost complete satellite system in the MATLAS survey, around the iconic NGC 474 galaxy, employing the Multi Unit Spectroscopic Explorer (MUSE) instrument mounted at the Very Large Telescope in Chile. We analyze the dwarfs by full spectrum fitting, which yields velocities, stellar metallicities and ages, and discuss the phase-space distribution of the satellite system in detail.

2. Data and methods

The NGC 474 group was selected as a follow up target because it was identified to host the most significant flattened distribution of dwarf galaxy candidates (Heesters et al. 2021) observable in the South during the semester P111. The data was acquired through the European Southern Observatory (ESO) programs 109.22ZV, 110.23QF.001, and 111.24KF (PI: Marleau) using the Multi Unit Spectroscopic Explorer (MUSE; Bacon et al. 2010, 2012) at UT4 of the Very Large Telescope (VLT) on Cerro Paranal, Chile. MUSE is an integral field unit (IFU) with an 1×1 arcmin^2 field of view, a spatial sampling of 0.2 arcsec/pixel, a nominal wavelength range of 480−930 nm, and a resolving power between 1740 (480 nm) and 3450 (930 nm). In total we observed 13 dwarf galaxy candidates from the MATLAS survey. We include three dwarf galaxies – MATLAS-20, MATLAS-29, and MATLAS-35 – that were already analyzed and presented in Heesters et al. (2023). In order to observe the major part of the galaxy (approx. to two effective radii) but have more clean sky, we applied an offset of the order of ±10 arcsec in RA and Dec from the center of the MUSE field of view. The MUSE data products are available through the ESO Science Archive, which includes the calibrated data run through the standard MUSE pipeline (Weilbacher et al. 2012, 2020). This included the bias and the flat-field correction, the astrometrical calibration, the sky-subtraction, and the wavelength and flux calibration (Hanuschik et al. 2017)[2].

For the sky subtraction, we directly used the data cube because the target dwarf galaxies are small enough that they leave enough space to estimate the sky. No sky exposures were taken. Müller et al. (2021b) estimated that with 20% of the MUSE field being free for the sky subtraction, better results are achieved when employing the science data cube instead of a sky offset. To further reduce the sky residual lines, we employed the Zurich Atmosphere Purge (ZAP) principal component analysis algorithm (Soto et al. 2016). To select the empty sky patches on the data we ran the python implementation of Source Extractor (Bertin & Arnouts 1996) called SEP (Barbary 2016) with a sigma threshold of 0.5, which creates a segmented fits file with all detected sources. This segmentation map served as mask for ZAP. We extracted the integrated spectra using an elliptical aperture, which was adjusted on the collapsed cubes. We again used SEP to mask foreground stars and background objects with different thresholds in a trial-by-error fashion. Additionally, we masked objects by hand where needed.

To extract the line-of-sight velocities and stellar population properties, we employed the Python implementation of the Penalized PiXel-Fitting (pPXF, Cappellari & Emsellem 2004; Cappellari 2017) algorithm. We followed the same steps as described in several previous studies employing MUSE and pPXF for this task (Emsellem et al. 2019; Fensch et al. 2019; Müller et al. 2020; Fahrion et al. 2020, 2022; Heesters et al. 2023). In summary, our approach involves utilizing a set of Single Stellar Population (SSP) spectra sourced from the eMILES library (Vazdekis et al. 2016), encompassing metallicities [M/H] spanning from solar levels down to −2.27 dex and ages ranging from 70 Myr to 14.0 Gyr. We adopt a Kroupa initial mass function (IMF, Kroupa 2001). The SSP library spectra undergo convolution with the line-spread function, following the methodology outlined in Guérou et al. (2017) and detailed in the Appendix of Emsellem et al. (2019). A variance spectrum is derived from the masked data cube and incorporated into pPXF to enhance the fitting process. For the kinematic fit, we employ 8 degrees of freedom for the multiplicative polynomial and 12 degrees for the additive polynomial (Emsellem et al. 2019). In the age and metallicity fits, we constrain the velocity, omit additive polynomials, and maintain the 12th degree in the additive polynomial (Fensch et al. 2019). We utilize pPXF weights to compute mean metallicities, mean ages, and stellar mass-to-light ratios from the SSP models for each galaxy. To enhance the fits, we mask residual sky lines not removed by ZAP. The spectra and the best-fit models of the confirmed NGC 474 members and background objects are presented in Figs. 1 and 2, and the derived properties are compiled in Tables 1 and 2.

The uncertainties on the best-fit parameters are estimated using a Monte Carlo method, where residuals are reshuffled in a bootstrap approach. The uncertainties are given as the 1σ standard deviation of the posterior distribution. We calculate the S/N ratio per pixel in a region between 6600 and 6800 Å, devoid of strong absorption or emission lines. This ratio is determined as the mean

[1] See http://obas-matlas.u-strasbg.fr/WP/, last accessed 30.01.2024.

[2] See also http://www.eso.org/observing/dfo/quality/PHOENIX/MUSE/processing.html

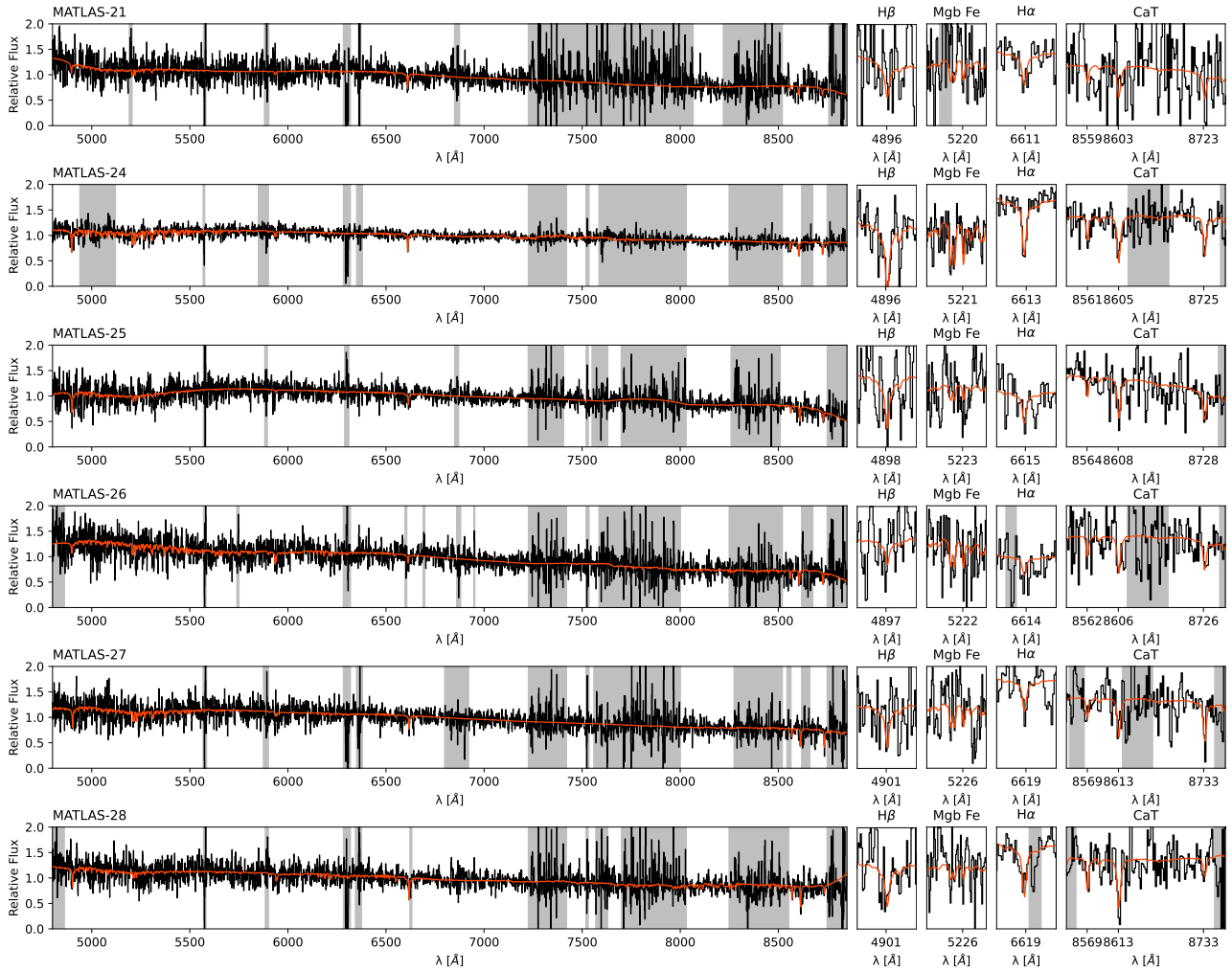

Fig. 1. Spectra of the confirmed dwarf galaxies in the field around NGC 474. The spectra (black line) and the best fit from pPXF (red line) is plotted in the left panel over the full spectral coverage of MUSE. The gray areas indicate masked regions. The right panels highlight features of interest that were relevant for the fitting.

fraction between flux and the square root of the variance, with the latter multiplied by the χ^2 value estimated by pPXF. Because the main goal of the observations was to measure the line-of-sight velocities, the targeted S/N ratio was 5. Therefore, we advise that the age and metallicity estimations to be taken with a precaution (e.g. Fahrion et al. 2019 argue that one needs a S/N ratio of >10 to determine a metallicity within 0.2 dex).

3. The mass-metallicity relation

The dwarf galaxies in the Local Group seem to follow a well defined relation in metallicity and mass (Kirby et al. 2013). Heesters et al. (2023) observed 56 dwarf galaxies from the MATLAS survey (Habas et al. 2020; Poulain et al. 2021) in different fields with MUSE using a similar data reduction pipeline as presented here[3]. They found an offset from this relation towards more metal-poor stellar populations, which they argue may be due to systematic differences in the estimation of the metallicity (coming from mainly CaT fitting of individual stars for the Local Group or full spectrum fitting for the whole galaxy for the MATLAS dwarfs). This begs the question whether we find a similar systematic difference with our new data. For that we show the mass-metallicity relation in Fig. 3 and compare it to the larger MATLAS dwarf sample and the Local Group dwarfs. Similar to Heesters et al. (2023), we find that in general the dwarfs from the MATLAS sample seem to be more metal poor than the Local Group dwarfs. We find four MATLAS dwarfs (MATLAS-19, MATLAS-21, MATLAS-25, and MATLAS-35) from our sample outside of the 3σ bounds defined by Kirby et al. (2013). This is not solely driven by the S/N ratio, because three of these dwarfs have a S/N ratio of ≈9−10, and only one has a low ratio of 5. The dwarfs studied here follow the same trend that was found in the previous MATLAS MUSE observations (Heesters et al. 2023) and may indicate a deviation from the mass-metallicity relation. Whether this is coming from differences in the measurement of the metallicity or rather has a physical nature remains to be seen.

4. The NGC 474 satellite system

Before we dive into the phase-space analysis of the NGC 474 system, we need a clear picture of the membership and satellite

[3] The main difference between the pipeline used here and from Heesters et al. (2023) is the extraction of the sky pixels using different tools, namely MTObject (Teeninga et al. 2015) or Source Extractor. This caused a difference in the stellar population properties for MATLAS-2019 between Heesters et al. (2023) and Müller et al. (2020), which was pointed out by Buzzo et al. (2024).

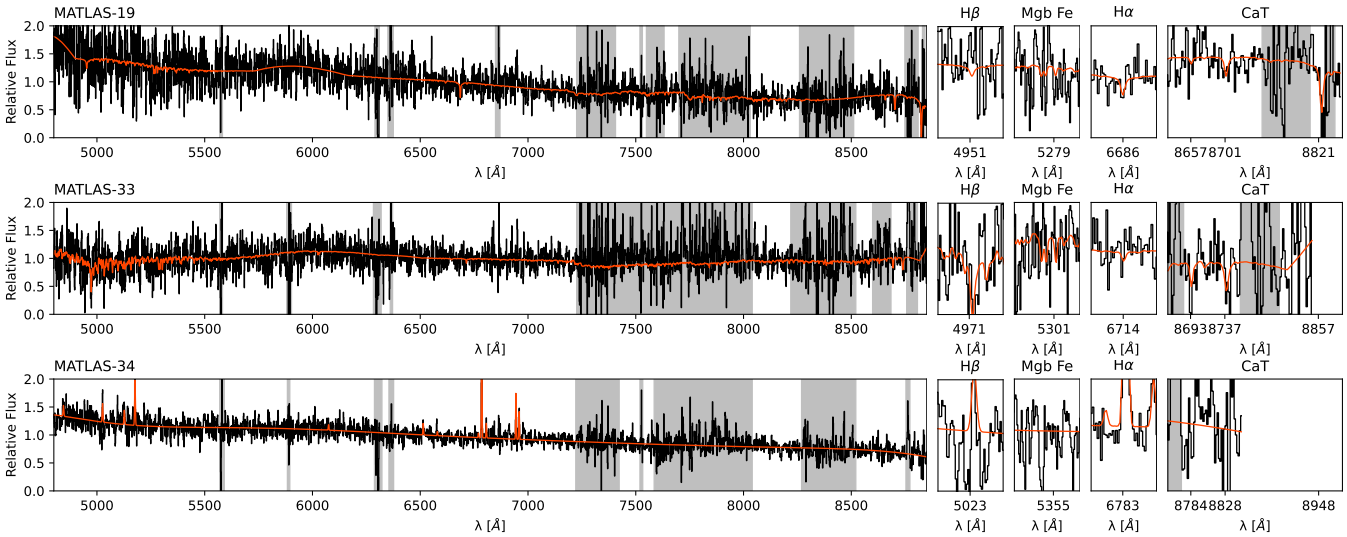

Fig. 2. Same as Fig. 1 but for the background galaxies.

Table 1. Confirmed NGC 474 dwarf galaxy system.

Name	RA	Dec	Exp. time	Vel.	[M/H]	Age	M/L	S/N	M_V
	deg	deg	s	km/s	dex	Myr	$M_\odot/L_\odot$		mag
(1)	(2)	(3)	(4)	(5)	(6)	(7)	(8)	(9)	(10)
MATLAS-20 [(a)]	19.584400	3.433197	2628	2409.0 ± 14.6	-1.70 ± 0.23	12.6 ± 1.5	2.2 ± 0.2	9.1	−12.2
MATLAS-21	19.594114	3.327721	5256	2161.9 ± 24.4	-2.16 ± 0.19	13.4 ± 2.1	2.0 ± 0.2	8.0	−12.3
MATLAS-24	19.848000	3.239670	2628	2216.8 ± 5.1	-1.36 ± 0.12	8.4 ± 1.9	1.6 ± 0.4	18.3	−13.0
MATLAS-25	19.858900	3.359683	2628	2339.6 ± 13.6	-1.90 ± 0.19	13.7 ± 2.6	1.8 ± 0.4	10.8	−12.8
MATLAS-26	19.930422	3.246573	2628	2263.8 ± 12.6	-1.36 ± 0.20	11.7 ± 2.1	2.0 ± 0.3	9.0	−12.3
MATLAS-27	20.062317	3.616693	2628	2500.1 ± 11.3	-1.52 ± 0.18	8.2 ± 2.3	1.5 ± 0.3	9.3	−12.7
MATLAS-28	20.119040	3.608794	5913	2508.2 ± 8.0	-1.5 ± 0.13	10.5 ± 2.3	1.8 ± 0.3	9.4	−12.4
MATLAS-29 [(a)]	20.146580	3.145582	2628	2153.4 ± 10.4	-1.62 ± 0.10	9.2 ± 2.0	1.9 ± 0.5	13.2	−13.7
MATLAS-35 [(a)]	20.494549	3.971204	2628	2193.8 ± 18.6	-2.14 ± 0.24	6.4 ± 3.8	1.2 ± 0.5	9.3	−12.9
LEDA 4765 [(b)]	19.909685	3.261206	–	2235 ± 31	–	–	–	–	
LEDA 1244578 [(b)]	19.965508	3.077404	–	2172 ± 16	–	–	–	–	−16.0

Notes. References for the values presented in this row are [(a)]Heesters et al. (2023), and [(b)]Rines et al. (2003). Some comments on the different columns: (4) the exposure time is the total integrated exposure time on target and may include several observing blocks. (8) The M/L ratio is the stellar mass-to-light ratio derived from the pPXF fitting of the spectrum. (9) The signal-to-noise is measured on the spectrum in a region between 6600 and 6800 Å. (10) Extinction corrected (Schlafly & Finkbeiner 2011) absolute magnitudes, estimated from the g and r band magnitudes of Poulain et al. (2021) for the MATLAS dwarfs, and Wang et al. (2018) for LEDA 1244578.

nature of the dwarf galaxies. But let us first assess the giant galaxies in the field.

The NGC 474 system includes the post-merger galaxy NGC 474 and close-by the spiral galaxy NGC 470 with a separation of ∼5.3 arcmin. Both have similar stellar masses with $6{-}9 \times 10^{10}\,M_\odot$ (Sheth et al. 2010; Cappellari et al. 2013) and $8 \times 10^{10}\,M_\odot$ (Sheth et al. 2010), respectively. In the further neighborhood, two other giant galaxies reside, namely NGC 488 and NGC 520, with separations of ∼1.9 deg and ∼1.2 deg with respect to NGC 474, respectively (see Fig. 4). At an adopted distance of 31 Mpc (Cappellari et al. 2011) for NGC 474[4], this translates into physical, projected separations of ∼50 kpc, ∼1000 kpc, and ∼650 kpc for NGC 470, NGC 488, and NGC 520, respectively. All galaxies share similar line-of-sight velocities, namely 2375 km/s for NGC 470 (Springob et al. 2005), 2315 km/s for NGC 474 (Cappellari et al. 2011), 2272 km/s for NGC 488 (Lu et al. 1993), and 2281 km/s for NGC 520 (Lu et al. 1993). Errors are between 1 and 5 km/s. The closeness in velocity space will make it difficult to disentangle membership of the dwarf galaxies based on their velocities alone. There are also two background galaxies within the projected virial radius of NGC 474, NGC 467 with a velocity of ∼5500 km/s (Huchra et al. 1999), and NGC 479 with a velocity of ∼5300 km/s (Yu et al. 2022). With such large differences in velocities to NGC 474, there is no confusion between their dwarf satellite members.

The MATLAS survey covered a $1.044 \times 1.153\,\mathrm{deg}^2$ field around NGC 474, which covers most of the virial radius (330 kpc, or ≈0.6 deg). We calculated the virial radius of the early-type galaxy NGC 474 using the abundance matching relation between the effective radius and R_{200} (Kravtsov 2013), with

[4] We note that several distance estimates exist based on different methods and calibrations (Cantiello et al. 2007; Cappellari et al. 2011; Tully et al. 2013), ranging between 28 and 33 Mpc. For consistency reason with other publications using the MATLAS data, we use the values provided by Cappellari et al. (2011).

Table 2. Rejected NGC 474 dwarf satellite candidates.

Name	RA	Dec	Exp. time	Vel.	[M/H]	Age	M/L	S/N	M_V
	deg	deg	s	km/s	dex	Myr	$M_\odot/L_\odot$		mag
(1)	(2)	(3)	(4)	(5)	(6)	(7)	(8)	(9)	(10)
MATLAS-19	19.558893	2.903885	5256	5576.0 ± 39.2	-2.25 ± 0.26	5.8 ± 2.0	1.12 ± 0.25	5.3	−13.0
MATLAS-23 [(c)]	19.711599	3.561740	–	4934 ± 8	–	–	–	–	−15.4
MATLAS-33	20.384933	3.671406	2628	6844.8 ± 19.6	-1.60 ± 0.24	9.7 ± 2.6	1.72 ± 0.36	6.1	−14.5
MATLAS-34 [(d)]	20.396175	3.563550	2628	9053.4 ± 36.1	–	–	–	10.3	−15.8

Notes. Same as Table 1. [(c)]MATLAS-23 was not observed with MUSE. Its velocity comes from ALFALFA HI observations (Yu et al. 2022). [(d)]The velocity is derived from emissions lines. (10) The distances are estimated from the Hubble flow using a Hubble constant of 70 km/s/Mpc.

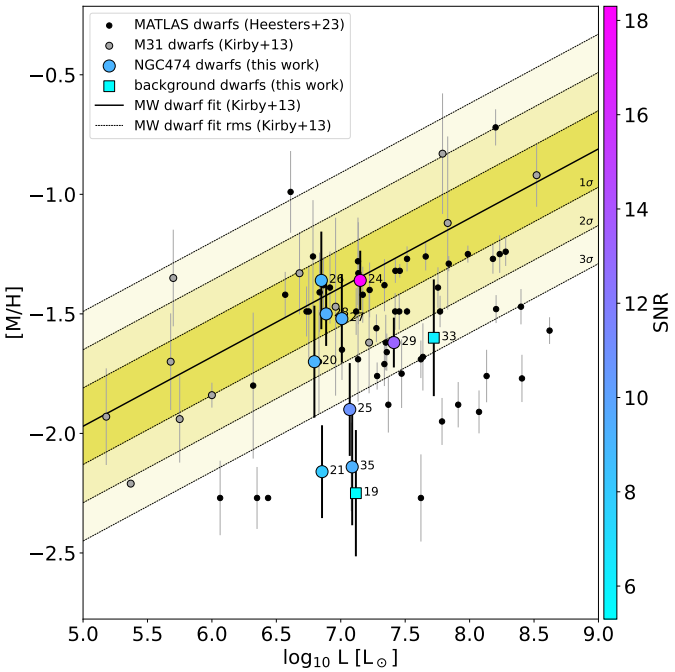

Fig. 3. Mass-metallicity relation for a reference sample of dwarf galaxies from the MATLAS survey (Heesters et al. 2023), the M31 dwarfs (Kirby et al. 2013), and the dwarf galaxies presented here. The black line corresponds to Eq. (3) from Kirby et al. (2013) and the yellow regions indicate the 1, 2, and 3σ intervals.

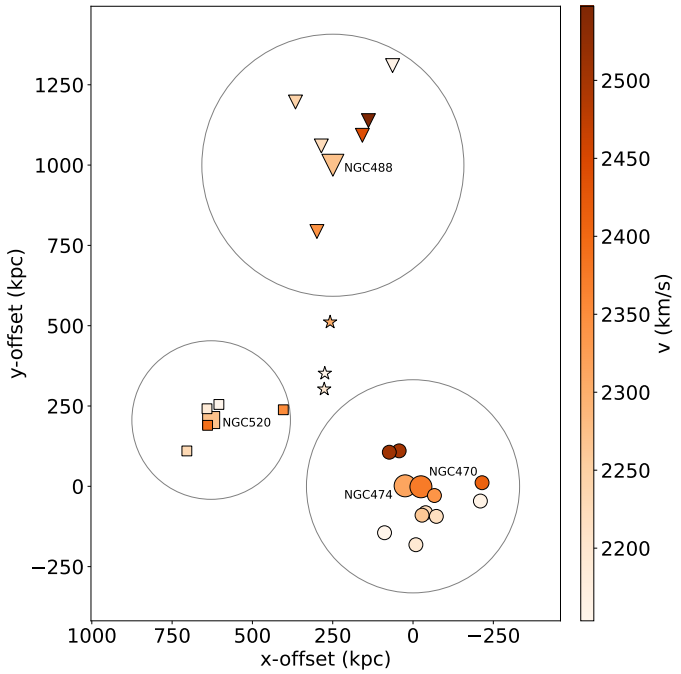

Fig. 4. Larger field in XY coordinates at a distance of 31 Mpc. The X-axis follows the RA-axis, with positive numbers towards East, the Y-axis follows the Dec-axis, with positive numbers towards North. Colors indicate the line-of-sight velocities. The circles correspond to the NGC 474/NGC 470 system, the squares to the NGC 520 system, and the triangles to the NGC 488 system. The stars indicate field dwarfs (being outside of the virial radius). The virial radii of the systems are indicated with gray circles.

an effective radius of 33 kpc (Cappellari et al. 2013). For the late-type galaxies shown in Fig. 4 we derive the virial radii from the baryonic masses and using Eq. (11) from McGaugh (2012), with a Hubble constant value of 70 km/s/Mpc. This calculation follows the baryonic Tully-Fisher relation as put forward in McGaugh (2012). We use an overdensity of $\Delta = 200$ above the cosmic density as definition for the virial mass and radius.

In the NGC 474 field there were 14 dwarf galaxy candidates listed in Poulain et al. (2021), Table 1. Additionally, there are two dwarf galaxies with known velocities, LEDA 4765 with $v = 2235 \pm 31$ km/s, and LEDA 1244578 with $v = 2172 \pm 16$ km/s (Rines et al. 2003) that are not in the MATLAS sample. If we are assuming that satellites have systemic velocities within ±300 km/s of their host galaxies (Habas et al. 2020), every dwarf galaxy candidate with a line-of-sight velocity between 2050 and 2650 km/s may potentially be a satellite member of the NGC 474 system. The central velocity of 2350 km/s is derived as a luminosity weighted mean between NGC 474 and NGC 470. We find that this is the case for nine of the observed dwarf galaxies, see Fig. 5. Four dwarf candidates (MATLAS-19, MATLAS-23, MATLAS-33, MATLAS-34, see Fig. 6) are actually background objects, we thus remove them from the satellite list[5]. See Table 2 for their velocities. This is consistent with the previous follow-up observations of MATLAS satellites, where a confirmation rate of 75% was found (Heesters et al. 2023). Here we report a confirmation rate of 70%. One dwarf galaxy candidate – MATLAS-22 – was not observed. We keep it in the list as a potential dwarf galaxy. Another dwarf – MATLAS-35 – is outside of the virial radius of NGC 474 and likely a field dwarf. This gives us a list of 10 confirmed dwarf satellite galaxies and one candidate in the NGC 474 system.

[5] MATLAS-19 and MATLAS-33 can be considered ultra-diffuse galaxies at their Hubble distance, with effective radii of 1.8 kpc, and 2.3 kpc, respectively.

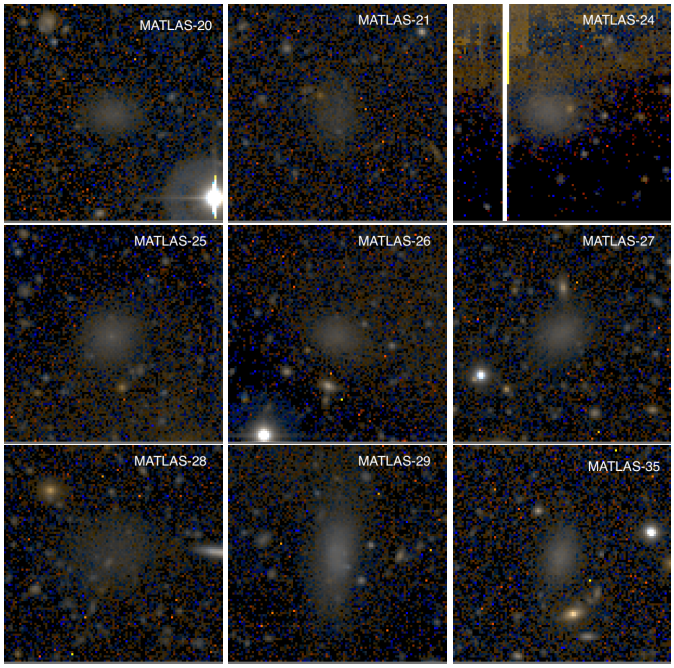

Fig. 5. Color-composite of the confirmed dwarf galaxies in the field surrounding NGC 474 from the MATLAS survey, processed from the MegaCam images and downloaded from the MATLAS webpage[1]. North to the top, East to the left. One side is one arcmin.

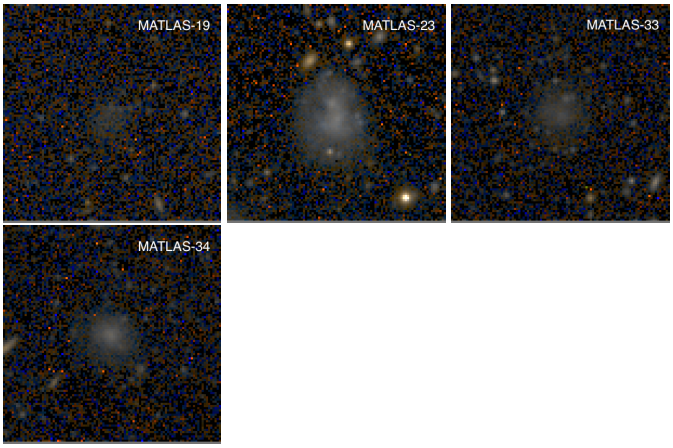

Fig. 6. Color-composite of the rejected dwarf galaxies of NGC 474 from the MATLAS survey, processed from the MegaCam images and downloaded from the MATLAS webpage. North to the top, East to the left. One side is one arcmin.

Two of the dwarf galaxies – MATLAS-27 and MATLAS-28 – share a very similar velocity (2500 ± 11 km/s and 2508 ± 8 km/s) and are close in projection with a separation of 3.45 arcmin (or 31 kpc at 31 Mpc). They may be a gravitationally bound pair of satellites. Are they massive enough to be physically bound? Geha et al. (2010) defined a criteria for a pair of satellites to be bound when

$$b \equiv 2GM_{\rm pair}/\Delta r \Delta v^2 > 1, \quad (1)$$

where Δr is the physical separation between the objects, Δv is their total velocity difference, $M_{\rm pair}$ is the total mass of the pair, and G is the gravitational constant. Because we do not have the total mass of the system, we can rephrase the question to how massive the system must be to be physically bound. The two dwarfs have stellar luminosities of 1.08×10^7 $L_\odot$ and 0.83×10^6 $L_\odot$, respectively (Poulain et al. 2021). This translates into masses of 1.6×10^7 $M_\odot$ for both using the measured stellar M/L ratio. If we solve for $M_{\rm pair}$ and using $\Delta r = 31$ kpc and $\Delta v = 8$ km/s we get a minimal total mass of the system of 2.3×10^8 $M_\odot$. The criteria $b > 1$ is satisfied by a total dark matter halo 7 times more massive than the stellar mass of the two combined (i.e. each dwarf has e.g. a mass-to-light ratio of 4). However, there are two problems: (a) the velocities have an uncertainty of ± 11 km/s which still allows for a large Δv, and (b) the true physical separation is unknown. A further assumption is that the tangential velocity vectors of the two dwarfs are similar or negligible. For (b) we can assume that the 3D separation is rather $\sqrt{2}$ times the projected separation (i.e. the uncertainty in depth is equal to the projected separation). If we assume $\Delta v = 16$ km/s (the quadratic sum of the two uncertainties and the absolute measured velocity difference) and $\Delta r = 44$ kpc we estimate a conservative total mass to be bound of 1.3×10^9 $M_\odot$. This is 41 times more massive than the combined stellar mass of the two. This would assume that the dwarfs have each a dark matter halo 20 times more massive than their stellar body, which for dwarf satellites in this luminosity range is reasonable (e.g., McConnachie 2012, and references therein). We thus argue that MATLAS-27 and MATLAS-28 could be a physically bound pair of satellites. Note that a dwarf galaxy satellite at this luminosity range typically resides in a stripped dark matter halo of the order of 10^9 to 10^{10} $M_\odot$ according to hydrodynamical simulations (Sales et al. 2022).

5. Spatial distribution

With the updated list of confirmed and rejected dwarf galaxy members of the NGC 474 group, we can study the spatial distribution of the satellite system. What is the overall flattening considering all dwarf galaxies within the virial radius? Applying a principal component analysis we recover a semi major axis of 105 kpc length and a minor-to-major axis ratio of 0.92. This is close to being round and quite different from a flattened distribution. Where is the difference to the previous study coming from?

Heesters et al. (2021) uses the Hough transform to find linear structures in data points, while simultaneously maximizing the number of data points in the linear structure and minimizing its thickness. Then they measured the flattening on the sub-population of dwarfs belonging to the linear structure. They found a planar structure with an rms length of 201 kpc and a rms height of 77 kpc, consisting of a sub-population of 13 out of the 14 dwarf candidates (effectively all the objects in their catalog belonged to their plane), which extended along the diagonal of the MATLAS footprint. This signal was mainly dominated by two dwarf galaxy candidates (MATLAS-19 and MATLAS-35) in the two opposing corners. Here we find that MATLAS-19 is actually a background object, and MATLAS-35 lies outside of the edge of the virial radius. The dwarf galaxy MATLAS-35 (top left in Fig. 7) is more distant compared to the other confirmed dwarf galaxies. With an angular separation of 42 arcmin, it is 380 kpc from NGC 474. This is almost the equidistant to NGC 520 (40 arcmin, see Fig. 4). This indicates that MATLAS-35 is not a satellite member, but resides in the larger field around NGC 474 (in its vicinity is another dwarf, see Fig. 4). For the other dwarf which drove the signal – MATLAS-19 – we now found based on the MUSE observations that it is not a member of the NGC 474 group at all, but that it rather is a background

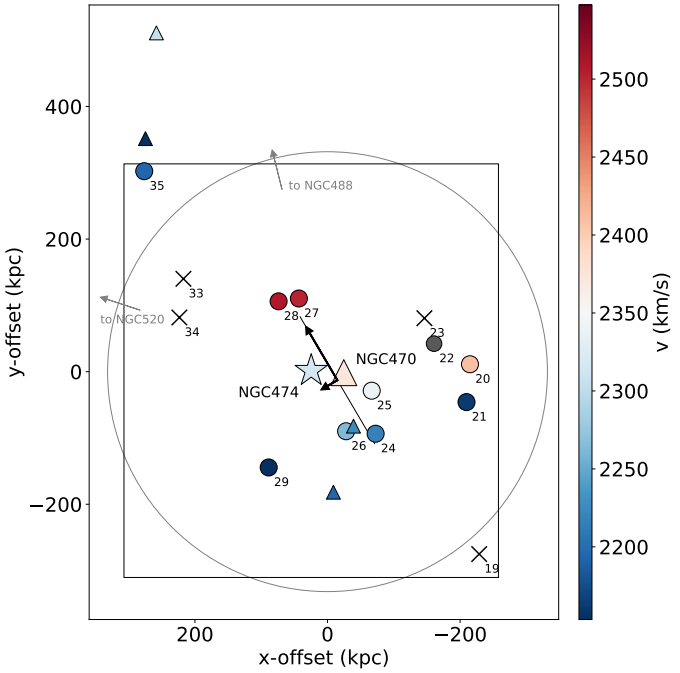

Fig. 7. Field in XY coordinates at a distance of 31 Mpc, with the field-of-view of the MATLAS survey indicated with the black rectangle. The X-axis follows the RA-axis, with positive numbers towards East, the Y-axis follows the Dec-axis, with positive numbers towards North. The small numbers indicate the MATLAS index of the dwarf, for example, 20 denotes MATLAS-20. Colors indicate the line-of-sight velocities, gray stands for no velocity measurement currently available. The large star and triangle are NGC 474 and NGC 470, respectively. The small triangles are known dwarfs in the field, the dots are the MATLAS dwarfs. Crosses are MATLAS candidates which are rejected as members of the NGC 474 group based on their velocities. The large gray circle indicates the virial radius. The line represents the linear substructure, arrows show the minor and major axis and their rms length and thickness.

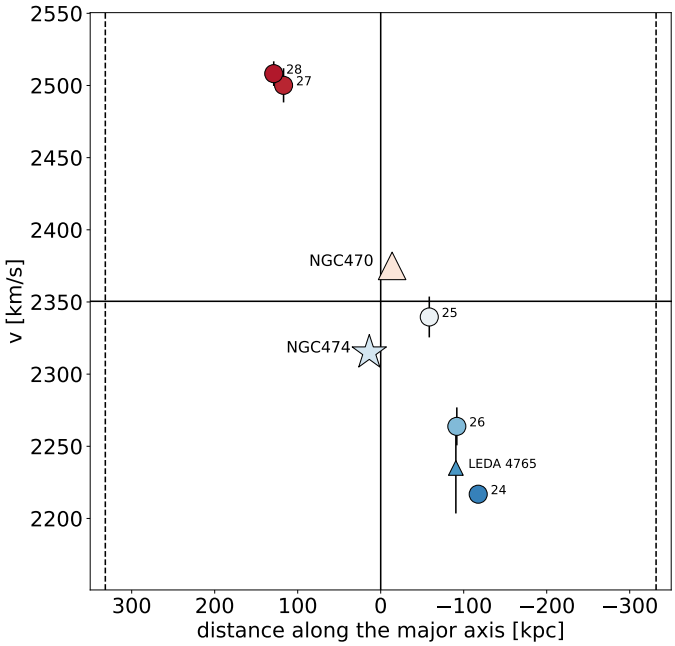

Fig. 8. Position velocity diagram. Same point and color scheme as in Fig. 7. The circles indicate dwarfs which are part of the identified linear-structure. Vertical dotted lines correspond to a virial radius of 230 kpc. The diagram is centered at the luminosity weighted mean velocity and position of NGC 474 and NGC 470.

galaxy. The updated membership list and restriction to objects within the virial radius therefore changes the estimated flattening of the dwarf galaxy system. However, there might be some interesting correlated sub-population in the data.

Applying the Hough transform to find linear structures, we find that six out of the eleven dwarf galaxies and candidate within the virial radius may belong to a linear structure. The center of the linear structure is between NGC 474 and NGC 470. The axis ratio is $b/a = 0.21$, with the semi minor axis rms length being $b = 24$ kpc and the semi major axis rms length $a = 111$ kpc, and includes MATLAS-24, MATLAS-25, MATLAS-26, MATLAS-27, MATLAS-28, and LEDA 4765. This is only a sub-population, containing half of the satellites of NGC 474. Looking at this sub-population, there seems to be a velocity trend (see Fig. 7 and next section). We note that for M 31 roughly half the dwarfs are in a planar structure (Ibata et al. 2013), however, the absolute number is higher (with 15 out of 27 satellites) and 3D information is available.

6. Kinematics

There is no clear central galaxy with both NGC 474 and NGC 470 having similar stellar masses. Therefore, we take the luminosity weighted mean velocity and position as the phase-space center of the group. This follows the approach of Müller et al. (2024) for the M 81/M 82 system. As discussed in the previous section, there is also no apparent flattening of the full satellite system. However, there seems to a sub-population of six dwarf satellites which seem to be phase-space correlated. Let us quantify this further.

If we calculate the distance Δ along the major axis of the Hough fit for the sub-population of the six dwarf galaxies, we can create a position-velocity diagram. As a convention, we assign a negative sign to galaxies occupying the Southern part of the structure. In Fig. 8 we plot the position-velocity diagram, together with the estimated virial radius. From the six dwarf galaxies five to six occupy two opposing quadrants, with one dwarf – MATLAS-25 – being ambiguous due to its uncertainty crossing the quadrants. Such a phase-space coherence may arise from co-rotation, however to confirm such an interpretation we would need both tangential and line-of-sight velocities. In general, if the system were fully pressure supported, all quadrants should be populated equally. If the system would be fully rotational supported, all satellites should occupy the two opposing quadrants.

The probability of finding the observed phase-space correlation – that is, estimating it as a fair coin flip – is 22%. This is calculated from the probability of getting 5 or 6 times the same result in a fair coin flip ($p = 0.5$), taking into account that we are agnostic on the side of the coin. It is fairly possible to get this result by chance. Getting six out of six (instead of at least five out of six) reduces the chance to 3%. Another way of studying the phase-space correlation of this sub-population is to calculate the Pearson correlation coefficient r. This coefficient measures a linear relationship in data points, with values ranging from -1 to 1. A Pearson r value close to 1 indicates a strong positive linear correlation, a value close to -1 indicates a strong negative linear correlation, and a value close to 0 indicates no linear correlation. For the sub-population of the six satellites, the Pearson r statistic

is 0.99, indicating a very strong positive correlation. The p-value is 0.00035. Assuming an α level of 0.01 to be statistically significant, this result is indeed significant.

The number of satellites for such tests is low, and the signal on one side from NGC 474 is only driven by two dwarf galaxies– which is likely a pair and do therefore not represent independent tracers. Such pairs can artificially boost the significance. Further caveats are that we only have access to line-of-sight velocities and projected positions, which may not represent the true 3D velocities and distribution of satellites. The two main galaxies NGC 474 and NGC 470 are rotating counter-wise to the satellite system.

7. Summary and conclusions

In this work, we have performed follow up observations with MUSE of the dwarf satellites of the NGC 474 system, previously discovered in the MATLAS survey. We could confirm nine dwarf galaxies to belong to the group and reject four as background objects. One other dwarf galaxy candidate still awaits spectroscopic follow-up.

Employing full spectrum fitting, we derived velocity and stellar body properties. The dwarfs are in general metal-poor and old. Compared to the Local Group dwarfs, they tend to be of lower metallicity, a finding which was previously reported on 56 MATLAS dwarf galaxies observed with MUSE.

In a recent work, Heesters et al. (2021) identified the NGC 474 system to host a significant flattened structure based on the distribution of the dwarf galaxy candidates. With the updated dwarf galaxy catalog, we reject their findings for this system. One of the main contributors to the identification of the flattened structure – MATLAS-19 – was found to be in the background and does not belong to the NGC 474 group, and another – MATLAS-35 – is outside of the virial radius. Using a Hough transformation to find linear structures, a flattened system of six dwarf galaxies may still be present in the data. When measuring the flattening of the overall system using its principle components, we find that the axis ratio changes from 0.2 (Heesters et al. 2021) to 0.9. We therefore conclude that there is no convincing evidence that all satellites form a plane-of-satellites as previously suggested.

However, we cannot rule out the possibility that a subpopulation of six dwarf galaxies may form a linear structure around the NGC 474/NGC 470 complex. We constructed a position velocity diagram to study any coherent motion within that sub-population. Out of six dwarf galaxies, five to six seem to coherently move (i.e. being redshifted on one side and blueshifted on the other side). With only six satellites, the signal is not conclusive. However, it is reminiscent of the pair-wise anti-correlated motions of satellites found in SDSS (Ibata et al. 2014b). These have been found to be a challenge for ΛCDM (Ibata et al. 2015, but see also Cautun et al. 2015b). Interestingly, the orientation of these pair-wise satellite seems to align with the large-scale environment (Ibata et al. 2014b).

Out of the 119 galaxy groups studied in the MATLAS survey with respect to their on-sky distribution, 31 were found to host a statistically significant flattened structure of dwarf galaxy candidates (Heesters et al. 2021). Here, we presented the first follow up of one of these significant groups and find that that previously proposed planar structure is not confirmed. Follow-up observations and a more systematic study of such systems would be key to be able to assess the agreement or disagreement with predictions from cosmological models.

Acknowledgements. We thank the referee for the constructive report, which helped to clarify and improve the manuscript. O.M. thanks Benoit Famaey for interesting discussions concerning the results by Ibata et al. (2014b). O.M. and N.H. are grateful to the Swiss National Science Foundation for financial support under the grant number PZ00P2_202104. M.S.P. acknowledges funding of a Leibniz-Junior Research Group (project number J94/2020). M.P. is supported by the Academy of Finland grant no: 347089. S.L. acknowledges the support from the Sejong Science Fellowship Program through the National Research Foundation of Korea (NRF-2021R1C1C2006790). R.H. acknowledges funding from the Italian INAF Large Grant 12-2022. S.P. acknowledges support from the Mid-career Researcher Program (No. RS-2023-00208957). This research was supported by the International Space Science Institute (ISSI) in Bern, through ISSI International Team project #534.

References

Bacon, R., Accardo, M., Adjali, L., et al. 2010, Proc. SPIE, 7735, 773508
Bacon, R., Accardo, M., Adjali, L., et al. 2012, The Messenger, 147, 4
Barbary, K. 2016, J. Open Source Softw., 1, 58
Bertin, E., & Arnouts, S. 1996, A&AS, 117, 393
Bílek, M., Duc, P.-A., Cuillandre, J.-C., et al. 2020, MNRAS, 498, 2138
Buck, T., Dutton, A. A., & Macciò, A. V. 2016, MNRAS, 460, 4348
Buzzo, M. L., Forbes, D. A., Jarrett, T. H., et al. 2024, MNRAS, 529, 3210
Cantiello, M., Blakeslee, J., Raimondo, G., Brocato, E., & Capaccioli, M. 2007, ApJ, 668, 130
Cappellari, M. 2017, MNRAS, 466, 798
Cappellari, M., & Emsellem, E. 2004, PASP, 116, 138
Cappellari, M., Emsellem, E., Krajnović, D., et al. 2011, MNRAS, 413, 813
Cappellari, M., Scott, N., Alatalo, K., et al. 2013, MNRAS, 432, 1709
Cautun, M., Bose, S., Frenk, C. S., et al. 2015a, MNRAS, 452, 3838
Cautun, M., Wang, W., Frenk, C. S., & Sawala, T. 2015b, MNRAS, 449, 2576
Chiboucas, K., Jacobs, B. A., Tully, R. B., & Karachentsev, I. D. 2013, AJ, 146, 126
Conn, A. R., Lewis, G. F., Ibata, R. A., et al. 2013, ApJ, 766, 120
Crosby, E., Jerjen, H., Müller, O., et al. 2023, MNRAS, 521, 4009
Danieli, S., van Dokkum, P., Conroy, C., Abraham, R., & Romanowsky, A. J. 2019, ApJ, 874, L12
Duc, P.-A., Cuillandre, J.-C., Karabal, E., et al. 2015, MNRAS, 446, 120
Emsellem, E., van der Burg, R. F. J., Fensch, J., et al. 2019, A&A, 625, A76
Fahrion, K., Lyubenova, M., van de Ven, G., et al. 2019, A&A, 628, A92
Fahrion, K., Müller, O., Rejkuba, M., et al. 2020, A&A, 634, A53
Fahrion, K., Bulichi, T.-E., Hilker, M., et al. 2022, A&A, 667, A101
Fensch, J., van der Burg, R. F. J., Jeřábková, T., et al. 2019, A&A, 625, A77
Fernando, N., Arias, V., Guglielmo, M., et al. 2017, MNRAS, 465, 641
Ferré-Mateu, A., Gannon, J. S., Forbes, D. A., et al. 2023, MNRAS, 526, 4735
Gámez-Marín, M., Santos-Santos, I., Domínguez-Tenreiro, R., et al. 2024, ApJ, 965, 154
Geha, M., van der Marel, R. P., Guhathakurta, P., et al. 2010, ApJ, 711, 361
Gillet, N., Ocvirk, P., Aubert, D., et al. 2015, ApJ, 800, 34
Guérou, A., Krajnović, D., Epinat, B., et al. 2017, A&A, 608, A5
Habas, R., Marleau, F. R., Duc, P.-A., et al. 2020, MNRAS, 491, 1901
Hanuschik, R., Data Processing, & Quality Control Group 2017, ESO Calibration Workshop: The Second Generation VLT Instruments and Friends, 15
Heesters, N., Habas, R., Marleau, F. R., et al. 2021, A&A, 654, A161
Heesters, N., Müller, O., Marleau, F. R., et al. 2023, A&A, 676, A33
Huchra, J. P., Vogeley, M. S., & Geller, M. J. 1999, ApJS, 121, 287
Ibata, R. A., Lewis, G. F., Conn, A. R., et al. 2013, Nature, 493, 62
Ibata, R. A., Ibata, N. G., Lewis, G. F., et al. 2014a, ApJ, 784, L6
Ibata, N. G., Ibata, R. A., Famaey, B., & Lewis, G. F. 2014b, Nature, 511, 563
Ibata, R. A., Famaey, B., Lewis, G. F., Ibata, N. G., & Martin, N. 2015, ApJ, 805, 67
Júlio, M. P., Pawlowski, M. S., Tony Sohn, S., et al. 2024, A&A, 687, A212
Kanehisa, K. J., Pawlowski, M. S., Müller, O., & Sohn, S. T. 2023, MNRAS, 519, 6184
Karachentsev, I. D., & Kroupa, P. 2024, MNRAS, 528, 2805
Kirby, E. N., Cohen, J. G., Guhathakurta, P., et al. 2013, ApJ, 779, 102
Koch, A., & Grebel, E. K. 2006, AJ, 131, 1405
Kravtsov, A. V. 2013, ApJ, 764, L31
Kroupa, P. 2001, MNRAS, 322, 231
Kroupa, P., Theis, C., & Boily, C. M. 2005, A&A, 431, 517
Libeskind, N. I., Cole, S., Frenk, C. S., Okamoto, T., & Jenkins, A. 2007, MNRAS, 374, 16
Libeskind, N. I., Hoffman, Y., Tully, R. B., et al. 2015, MNRAS, 452, 1052
Libeskind, N. I., Carlesi, E., Müller, O., et al. 2019, MNRAS, 490, 3786
Lu, N. Y., Hoffman, G. L., Groff, T., Roos, T., & Lamphier, C. 1993, ApJS, 88, 383

Lynden-Bell, D. 1976, MNRAS, 174, 695
Martínez-Delgado, D., Makarov, D., Javanmardi, B., et al. 2021, A&A, 652, A48
McConnachie, A. W. 2012, AJ, 144, 4
McConnachie, A. W., & Irwin, M. J. 2006, MNRAS, 365, 902
McGaugh, S. S. 2012, AJ, 143, 40
Metz, M., Kroupa, P., & Libeskind, N. I. 2008, ApJ, 680, 287
Müller, O., Jerjen, H., Pawlowski, M. S., & Binggeli, B. 2016, A&A, 595, A119
Müller, O., Scalera, R., Binggeli, B., & Jerjen, H. 2017, A&A, 602, A119
Müller, O., Pawlowski, M. S., Jerjen, H., & Lelli, F. 2018a, Science, 359, 534
Müller, O., Rejkuba, M., & Jerjen, H. 2018b, A&A, 615, A96
Müller, O., Rejkuba, M., Pawlowski, M. S., et al. 2019, A&A, 629, A18
Müller, O., Marleau, F. R., Duc, P.-A., et al. 2020, A&A, 640, A106
Müller, O., Pawlowski, M. S., Lelli, F., et al. 2021a, A&A, 645, L5
Müller, O., Fahrion, K., Rejkuba, M., et al. 2021b, A&A, 645, A92
Müller, O., Heesters, N., Pawlowski, M. S., et al. 2024, A&A, 683, A250
Mutlu-Pakdil, B., Sand, D. J., Crnojević, D., et al. 2024, ApJ, 966, 188
Paudel, S., Yoon, S.-J., & Smith, R. 2021, ApJ, 917, L18
Pawlowski, M. S. 2018, Mod. Phys. Lett. A, 33, 1830004
Pawlowski, M. S. 2021, Nat. Astron., 5, 1185
Pawlowski, M. S., & Kroupa, P. 2013, MNRAS, 435, 2116
Pawlowski, M. S., Pflamm-Altenburg, J., & Kroupa, P. 2012, MNRAS, 423, 1109
Pawlowski, M. S., Müller, O., Taibi, S., et al. 2024, A&A, 688, A153
Poulain, M., Marleau, F. R., Habas, R., et al. 2021, MNRAS, 506, 5494
Rines, K., Geller, M. J., Kurtz, M. J., & Diaferio, A. 2003, AJ, 126, 2152
Sales, L. V., Wetzel, A., & Fattahi, A. 2022, Nat. Astron., 6, 897
Santos-Santos, I., Gámez-Marín, M., Domínguez-Tenreiro, R., et al. 2023, ApJ, 942, 78
Sato, G., & Chiba, M. 2024, PASJ, 76, 498
Schlafly, E. F., & Finkbeiner, D. P. 2011, ApJ, 737, 103
Sheth, K., Regan, M., Hinz, J. L., et al. 2010, PASP, 122, 1397
Sohn, S. T., Patel, E., Fardal, M. A., et al. 2020, ApJ, 901, 43
Soto, K. T., Lilly, S. J., Bacon, R., Richard, J., & Conseil, S. 2016, MNRAS, 458, 3210
Springob, C. M., Haynes, M. P., Giovanelli, R., & Kent, B. R. 2005, ApJS, 160, 149
Taibi, S., Pawlowski, M. S., Khoperskov, S., Steinmetz, M., & Libeskind, N. I. 2024, A&A, 681, A73
Teeninga, P., Moschini, U., Trager, S. C., & Wilkinson, M. H. 2015, International Symposium on Mathematical Morphology and its Applications to Signal and Image Processing, Springer, 157
Tully, R. B., Courtois, H. M., Dolphin, A. E., et al. 2013, AJ, 146, 86
Tully, R. B., Libeskind, N. I., Karachentsev, I. D., et al. 2015, ApJ, 802, L25
Vazdekis, A., Koleva, M., Ricciardelli, E., Röck, B., & Falcón-Barroso, J. 2016, MNRAS, 463, 3409
Wang, J., Frenk, C. S., & Cooper, A. P. 2013, MNRAS, 429, 1502
Wang, L.-L., Luo, A. L., Shen, S.-Y., et al. 2018, MNRAS, 474, 1873
Weilbacher, P. M., Streicher, O., Urrutia, T., et al. 2012, Proc. SPIE, 8451, 84510B
Weilbacher, P. M., Palsa, R., Streicher, O., et al. 2020, A&A, 641, A28
Yu, N., Ho, L. C., Wang, J., & Li, H. 2022, ApJS, 261, 21